




Article

# *i*NOS Gene Ablation Prevents Liver Fibrosis in Leptin-Deficient *ob/ob* Mice

Sara Becerril <sup>1,2,3,\*</sup>, Amaia Rodríguez <sup>1,2,3</sup> , Victoria Catalán <sup>1,2,3</sup>, Beatriz Ramírez <sup>1,2,3</sup>,  
Xabier Unamuno <sup>1,2,4</sup>, Javier Gómez-Ambrosi <sup>1,2,3</sup>  and Gema Frühbeck <sup>1,2,3,5</sup> 

<sup>1</sup> Metabolic Research Laboratory, Clínica Universidad de Navarra, 31009 Pamplona, Spain; arodmur@unav.es (A.R.); vcatalan@unav.es (V.C.); bearamirez@unav.es (B.R.); xunamuno@unav.es (X.U.); jagomez@unav.es (J.G.-A.); gfruhbeck@unav.es (G.F.)

<sup>2</sup> CIBER Fisiopatología de la Obesidad y Nutrición (CIBEROBN), Instituto de Salud Carlos III, 28029 Madrid, Spain

<sup>3</sup> Obesity and Adipobiology Group, Instituto de Investigación Sanitaria de Navarra (IdiSNA), 31009 Pamplona, Spain

<sup>4</sup> Medical Engineering Laboratory, University of Navarra, 31009 Pamplona, Spain

<sup>5</sup> Department of Endocrinology & Nutrition, Clínica Universidad de Navarra, 31009 Pamplona, Spain

\* Correspondence: sbecman@unav.es; Tel.: +34-948-25-54-00 (ext. 5133); Fax: +34-948-29-65-00

Received: 15 January 2019; Accepted: 22 February 2019; Published: 27 February 2019



**Abstract:** The role of extracellular matrix (ECM) remodeling in fibrosis progression in nonalcoholic fatty liver disease (NAFLD) is complex and dynamic, involving the synthesis and degradation of different ECM components, including tenascin C (TNC). The aim was to analyze the influence of inducible nitric oxide synthase (*i*NOS) deletion on inflammation and ECM remodeling in the liver of *ob/ob* mice, since a functional relationship between leptin and *i*NOS has been described. The expression of molecules involved in inflammation and ECM remodeling was analyzed in the liver of double knockout (DBKO) mice simultaneously lacking the *ob* and the *i*NOS genes. Moreover, the effect of leptin was studied in the livers of *ob/ob* mice and compared to wild-type rodents. Liver inflammation and fibrosis were increased in leptin-deficient mice. As expected, leptin treatment reverted the obesity phenotype. *i*NOS deletion in *ob/ob* mice improved insulin sensitivity, inflammation, and fibrogenesis, as evidenced by lower macrophage infiltration and collagen deposition as well as downregulation of the proinflammatory and profibrogenic genes including *Tnc*. Circulating TNC levels were also decreased. Furthermore, leptin upregulated TNC expression and release via NO-dependent mechanisms in AML12 hepatic cells. *i*NOS deficiency in *ob/ob* mice improved liver inflammation and ECM remodeling-related genes, decreasing fibrosis, and metabolic dysfunction. The activation of *i*NOS by leptin is necessary for the synthesis and secretion of TNC in hepatocytes, suggesting an important role of this alarmin in the development of NAFLD.

**Keywords:** Leptin; *i*NOS; Tenascin C; liver fibrosis; inflammation

## 1. Introduction

Obesity is associated with a wide spectrum of liver abnormalities, including nonalcoholic fatty liver disease (NAFLD), characterized by an increased intrahepatic triglyceride content. NAFLD is a major contributor to cardiovascular disease and a major cause of obesity-related morbidity and mortality [1]. It represents the most prominent form of liver diseases worldwide and ranges from simple fatty liver and non-alcoholic steatohepatitis (NASH) to liver cirrhosis and hepatocellular carcinoma [2]. Although the cause of NAFLD is unclear, a “multiple-hit” model of NAFLD development has been postulated considering multiple insults acting together on genetically

predisposed subjects to develop NAFLD. Such hits include obesity, insulin resistance, hepatic lipid accumulation, activation of the inflammatory cascade, and fibrogenesis, as well as genetic and epigenetic factors [3]. Insulin resistance plays a key role, driving to an excessive de novo lipogenesis, a reduction of lipolysis, and the consequent increase of intrahepatic lipids [4]. Like other metabolic diseases, the generation of oxidative stress is another important contributor in the pathogenesis of NAFLD [5]. The excessive reactive oxygen species (ROS) participate in the development of NAFLD through different mechanisms, including lipid peroxidation and the subsequent activation of the nuclear transcription factor- $\kappa$ B (NF- $\kappa$ B) as well as the activation of hepatic stellate cells (HSC), the primary source of extracellular matrix (ECM) proteins such as collagen or tenascin C (TNC) [6]. NF- $\kappa$ B can bind to the inducible nitric oxide synthase (iNOS) promoter, inducing its expression and triggering the inflammatory process. The large amount of nitric oxide (NO) derived from iNOS stimulation acts in combination with ROS and produces nitrosative stress, creating a deleterious environment that leads to cell death and tissue damage [7].

Tenascin C is a multifunctional hexameric ECM glycoprotein undetectable in most healthy adult tissues, but highly expressed during embryonic development and dynamic tissue remodeling [8]. TNC modulates fibrotic and inflammatory responses in several diseases, including liver fibrosis, through the enhancement of the inflammatory response [9]. In this line, TNC is upregulated and deposited in both fibrotic areas and perisinusoidal spaces during liver diseases, with HSCs being considered its cellular source [10].

Leptin, the product of the *obese* (*ob*) gene, is also produced by HSCs after their activation [11]. In addition to its actions in the central nervous system, this adipocyte-derived hormone has direct effects on peripheral tissues, including the liver, the first adipokine directly associated with hepatic fibrosis [12]. Moreover, leptin mediates an inflammatory response by regulating the production of proinflammatory cytokines such as tumor necrosis factor alpha (TNF- $\alpha$ ), interleukin-6 (IL-6), and IL-1 $\beta$  [13]. These cytokines also increase the secretion of leptin, sustaining a chronic proinflammatory state [14].

The functional relationship between leptin and iNOS has been described earlier by our group [15–19] and others [20,21]. In order to delve into the knowledge about the functional interplay between leptin and iNOS, which we previously demonstrated in double knockout (DBKO) mice lacking both genes [18,22], we hypothesized that the *iNOS* gene is involved in the liver inflammation and fibrosis development of *ob/ob* mice.

## 2. Material and Methods

### 2.1. Animals

The generation of a DBKO mouse simultaneously lacking the *ob* and the *iNOS* genes was performed as previously described [18]. Briefly, male *ob/ob* mice were intercrossed with female *iNOS* knockout mice (*iNOS*<sup>-/-</sup>) on a C57BL/6J background (Jackson Laboratories, Bar Harbor, ME, USA). Male mice were weaned at 21 days of age, genotyped, and maintained at room temperature (RT) on an artificial light–dark cycle (lights on from 8:00 a.m. to 8:00 p.m.) with a relative humidity of 50  $\pm$  10% in a pathogen-free barrier facility. Mice had free access to water and were fed ad libitum a normal diet (ND) (12.1 kJ: 4% fat, 82% carbohydrate, and 14% protein, 2014S Teklad Global 14% Protein Rodent Maintenance Diet, Harlan, Barcelona).

In a second subset of experiments, ten-week-old *ob/ob* mice were subclassified into three groups: control, leptin-treated (1 mg/kg/d), and pair-fed ( $n = 5$  per group), as previously described [23]. The control and pair-fed groups received the vehicle (phosphate-buffered saline (PBS)), while leptin (Bachem, Bubendorf, Switzerland) was injected intraperitoneally twice a day at 8:00 a.m. and 8:00 p.m. for 28 days in the leptin-treated group. Control and leptin-treated groups were fed ad libitum with a standard chow diet (2014S Teklad, Harlan, Barcelona, Spain) [24], while the daily food intake of

the pair-fed groups was matched to the amount eaten by the leptin-treated groups the day before to discriminate the inhibitory effect of leptin on appetite.

Body weight and food intake were measured twice a week. The food efficiency ratio (FER) was determined as body weight gained per week divided by total energy (kcal) consumed over this period.

Twelve-week-old mice were sacrificed by CO<sub>2</sub> inhalation under fasting conditions. Sera samples were stored at −20 °C. Liver was carefully excised, weighed, frozen in liquid nitrogen, and stored at −80 °C. Hepatic biopsies were also fixed in 4% formaldehyde for immunohistochemical analyses. All experimental procedures conformed to the European Guidelines for the Care and Use of Laboratory Animals (Directive 2010/63/EU), and the study was approved by the Ethical Committee for Animal Experimentation of the University of Navarra.

## 2.2. Blood Measurements

Blood samples were collected by cardiac puncture. Serum glucose was measured using a blood glucose meter (Ascensia Elite, Bayer, Barcelona, Spain). Concentrations of triglycerides, free fatty acids (FFA) (Wako Chemicals GmbH, Neuss, Germany), and glycerol (Sigma, St. Louis, MO, USA) were measured by enzymatic methods using commercially available kits as previously described [18]. Serum insulin and adiponectin were determined by ELISA (Crystal Chem Inc., Chicago, IL, USA and BioVendor Laboratory Medicine Inc., Modrice, Czech Republic, respectively). Intra- and inter-assay coefficients of variation for measurements of insulin and adiponectin were, respectively, 3.5 and 6.3% for the former, and 5.6 and 7.2% for the latter. The homeostatic model assessment (HOMA) was calculated as an indirect measure of insulin resistance with the formula: [fasting insulin (μU/mL) × fasting glucose (mmol/L)]/22.5. Circulating levels of TNC were determined by ELISA (IBL International GmbH, Hamburg, Germany). Intra- and inter-assay coefficients of variation for measurements of TNC were 3.5 and 6.3%, respectively.

## 2.3. Intrahepatic Lipid Content

The intrahepatic triglyceride content was measured by enzymatic methods, as previously described [25]. Briefly, tissues were homogenized and diluted in saline at a final concentration of 50 mg/mL. Homogenates were diluted (1:1) in 1% deoxycholate (Sigma) and incubated at 37 °C for 5 min. For triglyceride measurements, samples were diluted 1:100 in the reagent (Infinity Triglycerides Liquid Stable Reagent, Thermo Electron Corporation, Louisville, CO, USA) and incubated for 30 min at 37 °C. The resulting dye was measured based on its absorbance at 550 nm. Concentrations were determined compared with a standard curve of triglycerides (Infinity™ Triglycerides Standard, Thermo Electron). The protein content of the homogenates was measured by the Bradford method, using bovine serum albumin (BSA) (Sigma) as standard. All assays were carried out in duplicate.

## 2.4. Cell Cultures

A non-tumorigenic mouse hepatocyte cell line AML12 was purchased from American Type Culture Collection (Manassas, VA, USA) and maintained in a DMEM/F-12 medium (Invitrogen, Barcelona Spain) supplemented with 10% fetal bovine serum (FBS) (Invitrogen), 5 μg/mL insulin, 5 μg/mL transferrin, 5 ng/mL selenium (Invitrogen), 40 ng/mL dexamethasone (Sigma), and antibiotic-antimycotic (complete growth medium). AML12 cells were plated  $2 \times 10^5$  cells/cm<sup>2</sup> and grown in complete growth medium. AML12 hepatic cells were serum-starved for 24 h, and quiescent cells were stimulated with recombinant murine leptin (10 nmol/L) (450-31, PeproTech EC Inc., Rocky Hill, NJ, USA) in the presence or absence of L-N<sup>6</sup>-(1-iminoethyl)-lysine (L-NIL), a specific NOS inhibitor (10 μmol/L) (I8021, Sigma). Moreover, AML12 hepatocytes were serum-starved for 24 h and quiescent cells were stimulated with recombinant tenascin C (10 nmol/L) (3358-TC-050; R&D Systems, Minneapolis, MN, USA). The concentrations of leptin, tenascin C, and pharmacological inhibitor to perform the experiments were chosen on the basis of previous studies carried out by

our group [22]. One sample per experiment was used to obtain control responses in the presence of the solvent.

### 2.5. RNA Extraction and Real-Time PCR

Total RNA was extracted from liver samples by homogenization with an ULTRA-TURRAX T 25 basic (IKA Werke GmbH, Staufen, Germany) using TRIzol Reagent (Invitrogen). RNA purification was carried out using the RNeasy Mini kit (Qiagen, Barcelona, Spain). All samples were treated with DNase (RNase-free DNase Set, Qiagen). The RNA concentration was determined from absorbance at 260 nm. For first-strand cDNA synthesis, constant amounts of total RNA were reverse transcribed using random hexamers as primers and M-MLV reverse transcriptase as previously described [26]. The transcript levels for *Tnc*, tumor necrosis factor- $\alpha$  (*Tnf*), toll-like receptor 4 (*Tlr4*), hypoxia inducible factor 1 alpha (*Hif1a*), CD11c (*Itgax*), *Cd44*, collagen type VI,  $\alpha 3$  (*Col6a3*), collagen type VI,  $\alpha 1$  (*Col6a1*), collagen type I,  $\alpha 1$  (*Col1a1*), egf-like module-containing mucin-like hormone receptor-like 1 (*Emr1*), matrix metalloproteinase 9 (*Mmp9*), transforming growth factor  $\beta$  (*Tgfb*),  $\alpha$  smooth muscle actin ( $\alpha$ -SMA, *Acta2*), and osteopontin (*Spp1*) were quantified by real-time PCR (7300 Real Time PCR System, Applied Biosystems, Foster City, CA, USA).

Primers and probes (Sigma) were designed using the software Primer Express 1.0 (Applied Biosystems) (Table S1). The cDNA was amplified at the following conditions: 95 °C for 10 min, followed by 45 cycles of 15 s at 95 °C and for 1 min at 59 °C, using the TaqMan Universal PCR Master Mix (Applied Biosystems). The primer and probe concentrations for gene amplification were 300 and 200 nmol/L, respectively. All results were normalized to the levels of 18S rRNA (Applied Biosystems), and the relative quantification was calculated using the  $\Delta\Delta C_t$  formula [27]. Relative messenger RNA (mRNA) expression was expressed as a fold expression over the calibrator sample. All samples were run in duplicate, and the average values were calculated.

### 2.6. Quantification and Characterization of Fibrotic Depots

Sections of formalin-fixed paraffin-embedded liver (6  $\mu$ m) were dewaxed with xylene and rehydrated with decreasing concentrations of ethanol. Fibrosis was localized by Sirius Red staining (Sigma). Images of five fields per section from each animal were obtained at 200 $\times$  magnification and the fibrous tissue area stained with Sirius Red/total amount of tissue was measured using the ImageJ analysis software, as described previously [28].

### 2.7. Statistical Analysis

Data are presented as the mean  $\pm$  SEM. Differences between groups were assessed by unpaired two-tailed Student's t-tests or two-way ANOVA as appropriate. In case of interaction between factors (lack of the *iNOS* or *ob* genes), a one-way ANOVA followed by Tukey's or least significant difference (LSD) post hoc tests were applied. Moreover, comparisons between *ob/ob* groups and controls were analyzed by one-way ANOVA followed by Tukey's post hoc tests. Statistics were calculated by the SPSS/Windows version 15.0 software (SPSS, Inc., Chicago, IL, USA). A *P*-value less than 0.05 was considered statistically significant.

## 3. Results

### 3.1. Lack of *iNOS* Gene Ameliorates the Obese Phenotype of *ob/ob* Mice

Anthropometric and metabolic variables of 12-week-old wild-type and leptin-deficient mice lacking the *iNOS* gene are shown in Table 1. As previously described [18,22], leptin-deficient *ob/ob* mice showed an increased ( $P < 0.001$ ) body and liver weight that was significantly reduced in the absence of the *iNOS* gene. The absence of the *ob* gene was associated with insulin resistance, reflected by the increased ( $P < 0.001$ ) levels of glucose, insulin, and HOMA index as well as by low adiponectin levels. Moreover, leptin deficiency was related with increased ( $P < 0.001$ ) serum levels of FFA and

glycerol. *iNOS* deficiency in *ob/ob* mice was associated with a significant improvement ( $P < 0.05$ ) in glucose and lipid metabolism as compared to *ob/ob* mice counterparts. The analysis of intrahepatic TG content also revealed that *iNOS* deletion significantly ( $P < 0.05$ ) decreased hepatosteatosis (Table 1).

**Table 1.** Anthropometric and metabolic characteristics of 12-week-old experimental animals.

	Wild Type	<i>iNOS</i> <sup>-/-</sup>	<i>ob/ob</i>	DBKO
Body weight (g)	24.0 ± 0.4	23.1 ± 0.4	44.9 ± 1.5	43.1 ± 0.8
Liver weight (g)	1.04 ± 0.02	1.00 ± 0.03	3.15 ± 0.12	2.97 ± 0.11
FFA (mmol/L)	0.74 ± 0.08	0.58 ± 0.03	1.07 ± 0.06 <sup>***</sup>	0.85 ± 0.06
TG (mg/dL)	66.3 ± 4.4	77.1 ± 3.9	97.3 ± 5.3 <sup>**</sup>	90.4 ± 0.1 <sup>†</sup>
Glycerol (mg/dL)	0.025 ± 0.001	0.022 ± 0.003	0.036 ± 0.001 <sup>***</sup>	0.030 ± 0.003 <sup>***, ††</sup>
Intrahepatic TG (mg/g)	19.0 ± 2.2	16.8 ± 1.5	28.5 ± 3.0	24.5 ± 2.6
Glucose (mg/dL)	83 ± 5	77 ± 2	410 ± 42 <sup>***</sup>	96 ± 5 <sup>***, ††</sup>
Insulin (ng/mL)	0.42 ± 0.04	0.32 ± 0.04	9.66 ± 0.61 <sup>***</sup>	8.89 ± 1.17 <sup>***, †††</sup>
HOMA	1.6 ± 0.2	1.1 ± 0.2	172.3.0 ± 21.5 <sup>***</sup>	34.5 ± 5.2 <sup>***, ††</sup>
Adiponectin (µg/mL)	22.6 ± 4.1	25.6 ± 3.1	16.6 ± 0.9 <sup>***</sup>	20.1 ± 5.0 <sup>***, ††</sup>

BW: body weight; DBKO: double knockout mice simultaneously lacking *ob* and *iNOS* genes; FFA: free fatty acids; HOMA: homeostasis model assessment; *iNOS*: Inducible nitric oxide synthase. TG: triacylglycerols. Data are mean ± SEM (n = 4–5 per group). Differences between groups were analyzed by two-way ANOVA or one-way ANOVA followed by Tukey's post hoc test when an interaction between factors was detected. \* $P < 0.05$ , \*\* $P < 0.01$ , \*\*\* $P < 0.001$  vs wild type mice; <sup>†</sup>  $P < 0.05$ , <sup>††</sup>  $P < 0.01$  vs *ob/ob* mice.

### 3.2. *ob/ob* Mice Lacking *iNOS* Display Changes in the Expression of Molecules Involved in Liver Inflammation

The gene expression levels of key molecules involved in the proinflammatory response were analyzed in the liver of the experimental animals. The mRNA levels of the murine macrophage markers *Itgax* and *Cd68*, as well as *Tnf* and *Hif1a* were upregulated in *ob/ob* mice and significantly downregulated in *iNOS* deficient mice as compared to those of wild-type mice (Figure 1a–d; Figure S1). Furthermore, the gene expression levels of *Emr1*, *Itgax*, *Cd68*, *Tnf*, and *Hifa* were significantly downregulated in DBKO mice simultaneously lacking *ob* and *iNOS* genes as compared to those of *ob/ob* mice, revealing decreased liver inflammation (Figure 1a–d; Figure S1).

Compelling evidence has demonstrated a close link between liver inflammation, the production of ECM, and the development of fibrosis [29]. Therefore, the hepatic expression of the alarmin TNC was analyzed in the context of leptin and *iNOS* deficiency. As shown in Figure 1e, leptin-deficient *ob/ob* mice exhibited a significant increase in *Tnc* gene expression levels compared to wild-type mice. Moreover, serum TNC levels were significantly increased ( $P < 0.05$ ) in *ob/ob* mice, and deletion of the *iNOS* gene reduced the circulating levels of this protein, confirming previous data described by our group (Figure 1f) [22].

Since TNC exhibits proinflammatory effects through the activation of TLR4, we compared the expression of genes involved in ECM remodeling in the absence of leptin and *iNOS*. Transcript levels of *Tlr4* were significantly ( $P < 0.05$ ) increased in the liver of leptin-deficient mice, whereas the deletion of the *iNOS* gene in *ob/ob* mice dramatically reduced its expression (Figure 2a). Furthermore, gene expression levels of collagen type VI (*Col6a1* and *Col6a3*) as well as collagen type I (*Col1a1*) were upregulated in the absence of leptin, while their increased expression was reverted in DBKO mice counterparts (Figure 2b–d), indicating that *iNOS* is responsible for the collagen production to a certain extent, resulting in less collagen accumulation in *iNOS*-deficient mice. The gene expression levels of the gelatinase *Mmp9* were also markedly decreased ( $P < 0.01$ ) in *iNOS* knockout and DBKO mice, whereas no differences were observed in *ob/ob* animals compared to wild-type mice (Figure 2e).

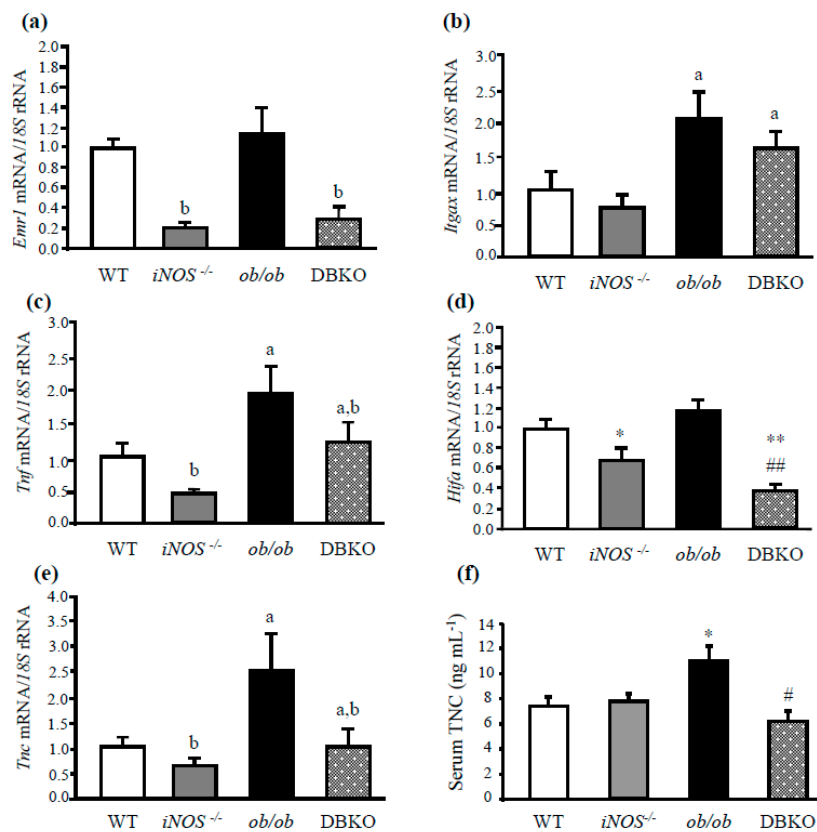


**Figure 1.** Hepatic expression of genes involved in inflammation and fibrosis. Gene expression levels of proinflammatory markers *Emr1* (a), *CD11c* (*Itgax*) (b), *Tnf* (c), *Hif1a* (d), and tenascin C (*Tnc*) (e) in the liver ( $n = 5-6$ ). The gene expression in wild type (WT) mice was assumed to be 1. Serum TNC levels (f) of the different experimental groups ( $n = 5$  per group). Differences between groups were analyzed by two-way ANOVA or one-way ANOVA followed by Tukey's post hoc test when an interaction between factors was detected. <sup>a</sup> $P < 0.05$  effect of the absence of the *ob* gene. <sup>b</sup> $P < 0.05$  effect of the absence of the *iNOS* gene. \* $P < 0.05$ , \*\* $P < 0.01$  vs WT mice; # $P < 0.05$ , ## $P < 0.01$  vs *ob/ob* mice. *iNOS*: Inducible nitric oxide synthase; DBKO: double knockout.

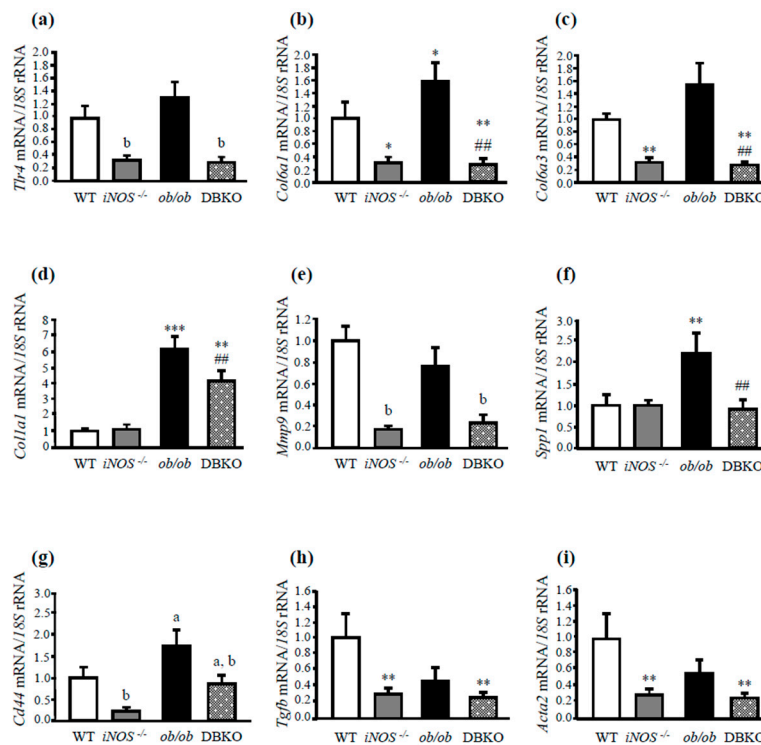


**Figure 2.** Effect of the absence of the *iNOS* gene in liver fibrosis in the context of leptin deficiency. Gene expression levels of *Tlr4* (a), *Col6a1* (b), *Col6a3* (c), *Col1a1* (d), *Mmp9* (e), *Spp1* (f), and *Cd44* (g) in the liver. Gene expression levels of liver *Tgfb* (h) and  $\alpha$ -SMA (*Acta2*) (i) ( $n = 5$ ) were also analyzed. The gene expression in WT mice was assumed to be 1. Differences between groups were analyzed by two-way ANOVA or one-way ANOVA followed by Tukey's post hoc test when an interaction between factors was detected. <sup>a</sup> $P < 0.05$  effect of the absence of the *ob* gene. <sup>b</sup> $P < 0.05$  effect of the absence of the *iNOS* gene. \* $P < 0.05$ , \*\* $P < 0.01$ , \*\*\* $P < 0.001$  vs WT mice; ## $P < 0.01$  vs *ob/ob* mice.

We next analyzed gene expression levels of osteopontin (*Spp1*), a multifunctional protein involved in liver diseases. *Spp1* mRNA significantly increased ( $P < 0.001$ ) in leptin-deficient mice (Figure 2f). Moreover, gene expression levels of the osteopontin receptor CD44, recently described as an important marker and a key player of liver diseases, including NAFLD [30], were also determined. Leptin deficiency was associated with higher hepatic *Cd44* mRNA, while the deletion of *iNOS* significantly decreased ( $P < 0.05$ ) its transcription levels (Figure 2g).

Gene expression levels of the profibrogenic TGF- $\beta$  were also analyzed. Deletion of *iNOS* significantly decreased ( $P < 0.01$ ) *Tgfb* mRNA expression levels (Figure 2h). In order to elucidate the regulatory effect of the absence of the *ob* and *iNOS* genes in the activation of HSC,  $\alpha$ -SMA (*Acta2*) gene expression levels were also determined. mRNA *Acta2* was dramatically downregulated ( $P < 0.01$ ) after *iNOS* deletion (Figure 2i). Notably, a significant correlation between hepatic gene expression levels of *Tnc* and *Tlr4* ( $r = 0.442$ ;  $P = 0.045$ ) as well as with *Tnf* ( $r = 0.67$ ;  $P = 0.001$ ), *Col6a1* ( $r = 0.36$ ;  $P = 0.048$ ), *Col6a3* ( $r = 0.66$ ;  $P = 0.001$ ), *Col1a1* ( $r = 0.56$ ;  $P = 0.008$ ), *Acta2* ( $r = 0.68$ ;  $P = 0.001$ ), and *Tgfb* ( $r = 0.49$ ;  $P = 0.023$ ) was found.

### 3.3. Leptin Administration Protects from Inflammation and Fibrosis in the Liver of *ob/ob* Mice

The anthropometric and metabolic characteristics of *ob/ob* mice after leptin replacement or pair-feeding are reported in Table S2. As expected, leptin administration ameliorated the obese and diabetic phenotype as well as improved lipid metabolism of *ob/ob* mice, corroborating previous findings of our group [22,31] and others [32,33]. Moreover, the increased liver weight observed in the absence of leptin was reversed ( $P < 0.001$ ) by either caloric restriction or leptin replacement. The histological examination supported the results of the serum biochemical analysis: *ob/ob* liver sections

exhibited macrovesicular steatosis that was completely reversed after leptin administration for 28 days, but not by caloric restriction (Figure 3a and Table S2).

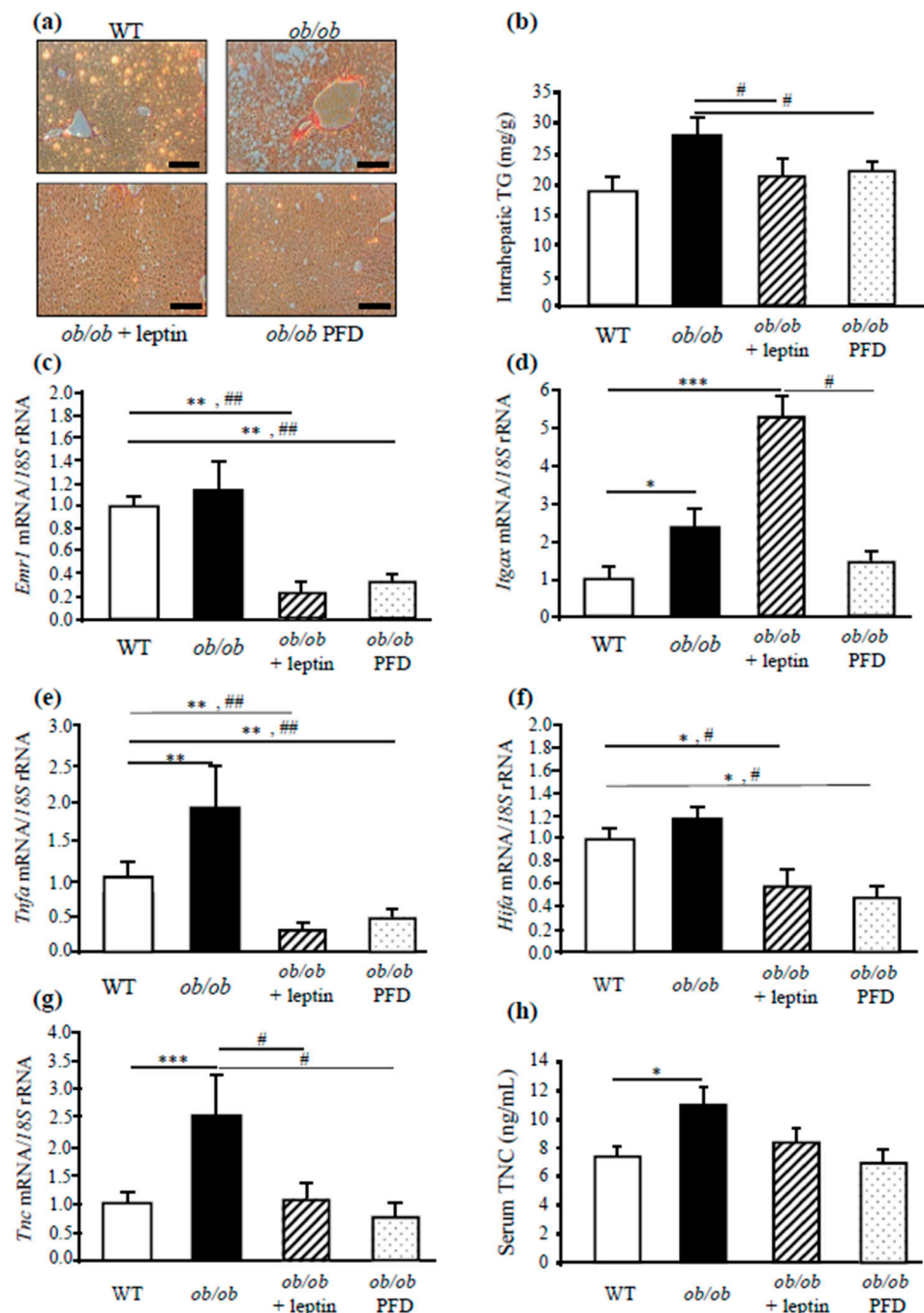


**Figure 3.** Effect of in vivo leptin administration on the liver phenotype and expression of genes involved in hepatic inflammation in *ob/ob* mice. Representative Sirius Red staining (magnification 200 $\times$ , scale bar = 50  $\mu$ m, n = 3/per group) (a) and intrahepatic TG content (n = 4–5 per group) (b). Gene expression levels of *Emr1* (c), *CD11c* (*Itgax*) (d), *Tnfa* (e), *Hif1a* (f), and *Tnc* (g) in the liver (n = 5–6) in wild-type (WT), *ob/ob*, leptin-treated, and pair-fed *ob/ob* mice (n = 5–6 per group). Gene expression levels in WT mice in liver were assumed to be 1. Serum TNC levels (h) of the different experimental groups (n = 5 per group). Comparisons between *ob/ob* groups and controls were analyzed by one-way ANOVA followed by Tukey's post hoc tests. \* $P$  < 0.05, \*\* $P$  < 0.01, \*\*\* $P$  < 0.001 vs WT mice; # $P$  < 0.05, ## $P$  < 0.01 vs *ob/ob* mice. PFD: Pair-fed group.



The influence of leptin deficiency in liver fibrosis was next investigated. Analysis of Sirius Red-stained sections revealed that, in the control group of WT mice, staining was only observed in areas surrounding the blood vessels, whereas in *ob/ob* mice a slight intralobulillar liver fibrosis was observed. Liver fibrosis was less evident after leptin administration and caloric restriction (Figure 3a). Moreover, as shown in Figure 3b, *ob/ob* mice exhibited higher hepatic TG content, with the leptin administration and caloric restriction decreasing ( $P < 0.05$ ) intrahepatic TG.

The inflammatory and fibrotic condition was also reversed in leptin-treated and pair-fed *ob/ob* mice, as evidenced by the decreased ( $P < 0.05$ ) mRNA levels of factors related with the proinflammatory response, including *Emr1*, *Itgax*, *Tnfa*, *Hifa*, and *Tnc* (Figure 3c–g). Serum TNC levels were also normalized after leptin administration (Figure 3h). Moreover, it was also observed that leptin administration, as well as pair-feeding of *ob/ob* mice, prevented the increased mRNA expression of genes related to ECM remodeling such as *Tlr4*, *Col6a1*, *Col6a3*, *Col1a1*, *Mmp9*, and the marker of liver injury *Cd44*, the profibrogenic *Tgfb*, and the marker of activated of HSCs *Acta2* (Figure 4a–h). These data support the idea that the obese state is strongly associated with the inflammatory response and the extracellular matrix remodeling.

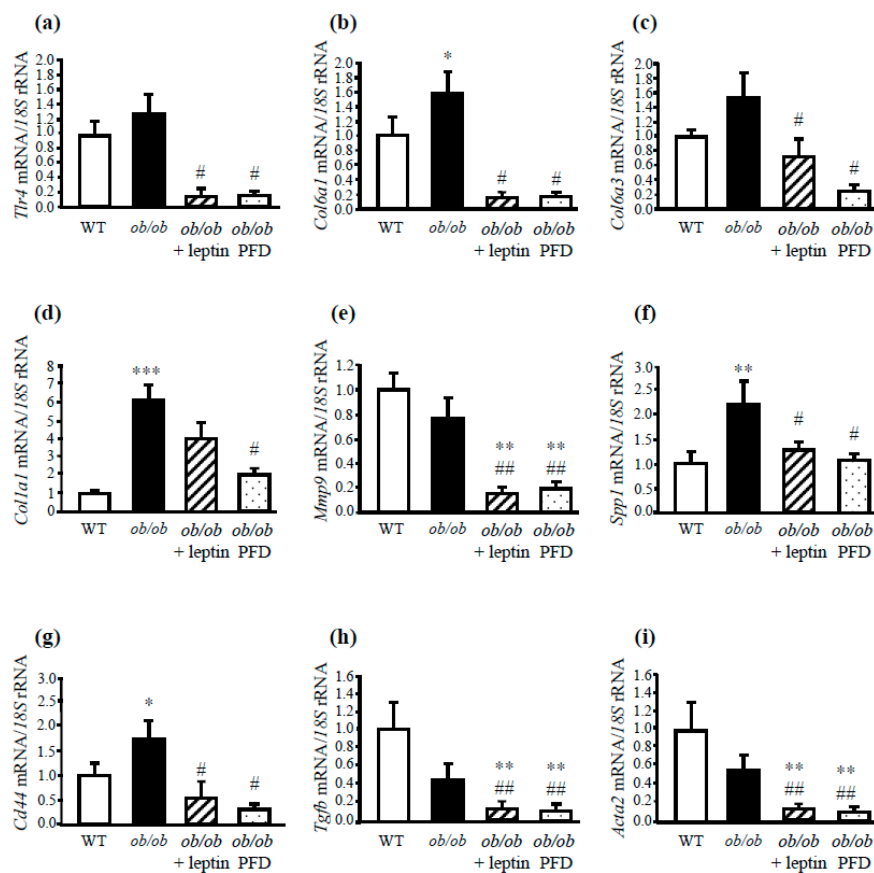


**Figure 4.** Effect of leptin replacement on the expression of genes involved in liver fibrosis in *ob/ob* mice. Gene expression levels of *Tlr4* (a), *Col6a1* (b), *Col6a3* (c), *Col1a1* (d), *Mmp9* (e), *Spp1* (f), and *Cd44* (g) in the liver of WT, *ob/ob*, leptin-treated, and pair-fed *ob/ob* mice ( $n = 5-6$  per group). Gene expression levels of *Tgfb* (h) and  $\alpha$ -SMA (*Acta2*) (i) were also evaluated. Gene expression levels in WT mice were assumed to be 1. Comparisons between *ob/ob* groups and controls were analyzed by one-way ANOVA followed by Tukey's post hoc tests. \* $P < 0.05$ , \*\* $P < 0.01$ , \*\*\* $P < 0.001$  vs WT mice; # $P < 0.05$ , ## $P < 0.01$  vs *ob/ob* mice.

### 3.4. Leptin Treatment Increases Inflammatory and Fibrotic Genes in AML12 Hepatocytes

The direct effect of leptin treatment on the expression of inflammatory and fibrogenic genes was demonstrated in vitro using the non-tumorigenic mouse hepatocyte AML12 cell line. Upon 24 h leptin stimulation at physiological concentrations (10 nmol/L), *Hif1a* mRNA expression was significantly upregulated ( $P < 0.05$ ), and the gene expression levels of *Mmp9* and *Tlr4*, although differences were not statistically significant ( $P = 0.103$  and  $P = 0.150$ , respectively) (Figure 5a–c). As expected, the expression of *Emr1* was not detected in AML12 hepatic cells (data not shown). Remarkably, leptin administration in AML12 hepatocytes significantly increased ( $P < 0.01$ ) the expression of one of the most potent profibrogenic cytokine *Tgfb*, producing also a tendency towards an increased  $\alpha$ -SMA (*Acta2*) gene expression ( $P = 0.150$ ) (Figure 5d,e). Furthermore, leptin treatment upregulated the transcription of the *Tnc* gene ( $P = 0.09$ ) with a significantly increased ( $P < 0.05$ ) release of TNC (Figure 5f,g).

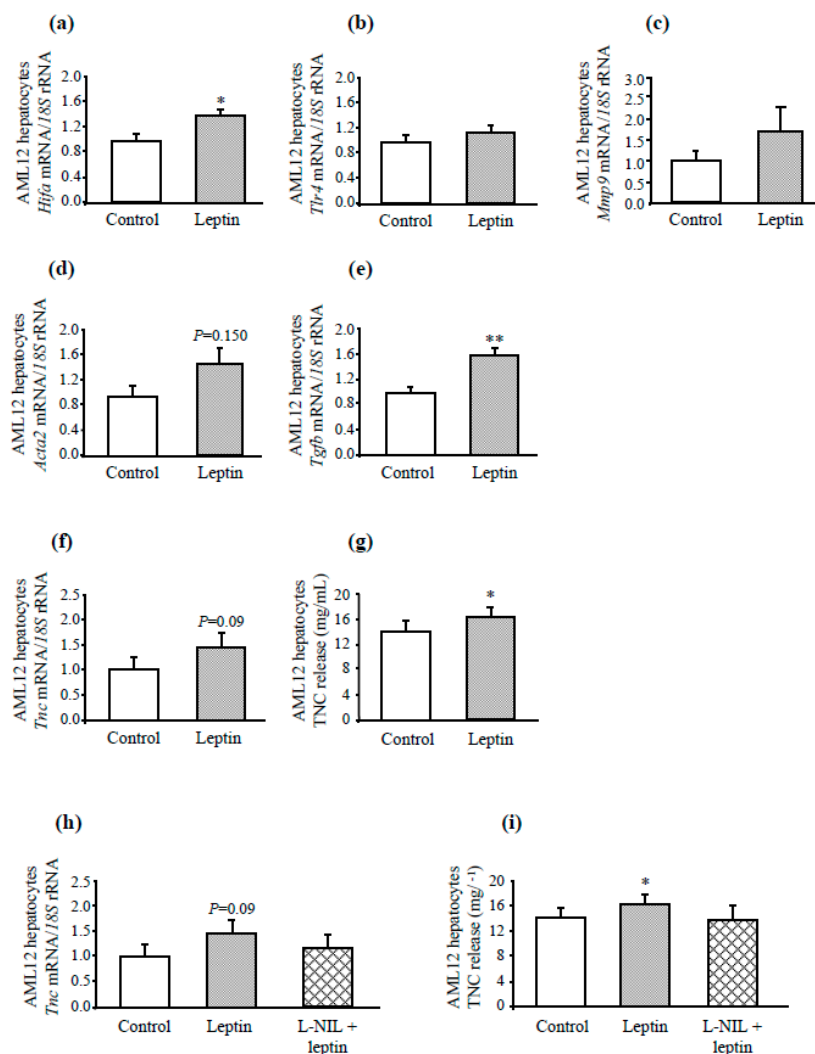


**Figure 5.** Effect of leptin stimulation for 24 h on the expression of markers of inflammation and fibrosis in AML12 hepatocytes. Effect of leptin stimulation (10 nmol L<sup>-1</sup>) for 24 h on gene expression levels of *Hif1a* (a), *Tlr4* (b), *Mmp9* (c),  $\alpha$ -SMA (*Acta2*) (d), *Tgfb* (e), and *Tnc* (f) as well as TNC release to the culture media (g) in AML12 liver cells (n = 6 per group). *Tnc* transcript levels (h) and TNC release (i) to the culture media in AML12 adipocytes stimulated with leptin (10 nmol/L) in the absence or presence of the iNOS inhibitor L-NIL (10 mmol/L) for 24 h. Gene expression levels in the unstimulated cells were assumed to be 1. Values are the mean  $\pm$  SEM (n = 5 per group). Differences between groups were analyzed by unpaired two-tailed Student's *t*-tests. \* $P < 0.05$ ; \*\* $P < 0.01$  vs unstimulated cells.

In order to determine the contribution of iNOS in mediating leptin-induced inflammation in AML12 hepatocytes, the effect of the pharmacological inhibition of iNOS with L-NIL, a selective iNOS inhibitor, was analyzed. Pharmacological inhibition of iNOS blunted the leptin-induced increase in *Tnc* mRNA after leptin stimulation as well as TNC release to the control media (Figure 5h,i). These results directly demonstrate the contribution of iNOS in *Tnc* expression in hepatic cells.

The stimulation with TNC significantly increased the expression levels of genes *Tlr4*, *Hif*, *Col6a1*, and *Col6a3* ( $P < 0.05$ ) as well as *Tnf* ( $P = 0.08$ ) in AML12 hepatic cells, without differences in *Mmp9* gene expression levels (data not shown) (Figure 6a–e), corroborating that this alarmin can induce a potent fibrogenic response. Noteworthy, TNC stimulation significantly increased the expression of both *Tgfb* and *Acta2* ( $P < 0.05$ ) (Figure 6f,g).

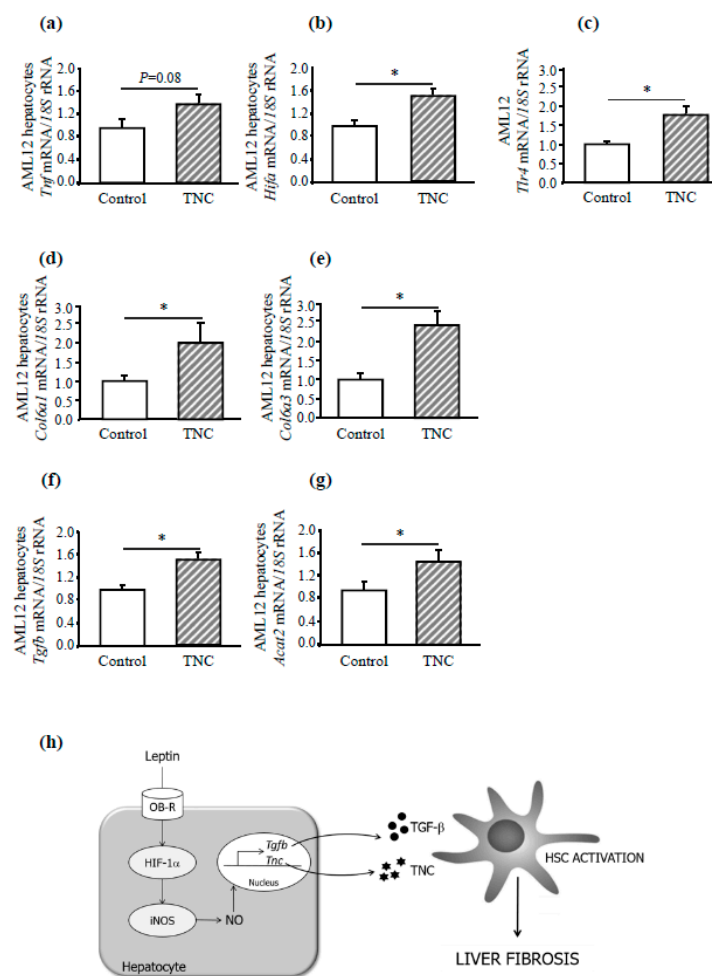


**Figure 6.** Effect of tenascin C (TNC) stimulation for 24 h on the expression of markers of inflammation and fibrosis in AML12 hepatocytes. Effect of TNC stimulation (10 nmol/L) for 24 h on gene expression levels of *Tnfa* (a), *Hif1a* (b), *Tlr4* (c), *Col6a1* (d), *Col6a3* (e), as well as *Tgfb* (f) and *a-SMA* (*Acta2*) (g) in AML12 hepatocytes ( $n = 5$  per group). Differences between groups were analyzed by unpaired two-tailed Student's *t*-tests. \* $P < 0.05$  vs unstimulated cells. Summary graph for the regulation of liver fibrosis induced by leptin through iNOS activation (h).

#### 4. Discussion

Adipose tissue is not only involved in energy storage but also functions as an endocrine organ secreting different bioactive adipokines [13,34]. The proinflammatory adipokine leptin regulates body weight and metabolism, exerting pleiotropic effects in many physiological systems including the liver, thereby linking obesity, insulin resistance, type 2 diabetes, and NAFLD [35–37]. Despite the wide range

of reports regarding the participation of leptin in inflammation, its role in the pathogenesis of NAFLD remains unclear. However, increased serum leptin levels have been correlated with the amount of inflammation and fibrosis in liver diseases [38]. One of the key events in the promotion of liver diseases is the activation of HSCs [29]. Activated HSCs are the primary source of extracellular matrix components such as collagen or TNC, and accordingly fibrosis. Activated HSCs also express leptin, pointing to the implication of this factor during hepatic fibrogenesis and disease progression [11]. Moreover, our results also showed that leptin significantly and directly increased the proliferation of HSCs in a dose-dependent manner, confirming the ability of leptin to stimulate HSCs by the increased *Acta2* mRNA levels, a marker of HSC activation [39], in AML12 hepatic cells. Moreover, upon 24 h leptin stimulation, AML12 hepatocytes increased the expression of *Tgfb1*, considered a key driver in the activation of HSCs [40]. These results suggest that leptin, produced by HSC, increases *Tgfb1* expression, which, in turn, stimulates fibrogenesis in HSC in an intricate paracrine loop. Furthermore, the pro-inflammatory capacity of leptin promotes or sustains low-grade inflammation [41,42]. In this context, leptin administration increases both inflammation and fibrogenesis in AML12 hepatocytes. Leptin also stimulated the synthesis and release of TNC in the liver, which interacts with several ECM proteins and cell receptors, including TLR4. TLRs are not only important in the regulation of innate and adaptive immune responses, but they are also involved in inflammatory diseases of the cardiovascular system and liver [43]. The TNC/TLR4 signaling axis is fundamental for the induction of proinflammatory cytokines and the ECM remodeling, among other functions [44]. In this regard, our group has recently reported that TNC, through TLR4, is implicated in the etiopathology of obesity adipose tissue inflammation [22]. Several studies support that TNC is involved in liver fibrosis, in part due to its distribution in areas of lymphocytic infiltration, contributing to liver fibrogenesis through the enhancement of the inflammatory response, the promotion of HSC activation, and the enhancement of TGF- $\beta$  expression [9]. In order to determine if TNC induces potent fibrotic and inflammatory responses not only in fibroblasts [45] but also in hepatocytes, AML12 cells were stimulated with this alarmin. The stimulation of murine AML12 hepatocytes with TNC increased the expression of *Tlr4*, *Hif1a*, *Tnfa*, and the fibrogenic genes *Col6a1* and *Col6a3*, confirming the important role of TNC in both liver fibrogenesis by increasing the synthesis of collagen and in the hepatic inflammatory response.

Converging lines of evidence have demonstrated that leptin exerts a regulatory role in the connection between energy metabolism and the immune system, being a crucial adipokine responsible for the inflammatory state found in obesity [46]. Leptin-deficient *ob/ob* mice exhibited increased liver inflammatory and fibrotic response, as evidenced by the increased infiltration of liver macrophages, collagen production, and fibrotic matrix deposition. In this context, hypoxia is considered another key microenvironmental factor contributing to inflammation and fibrosis in liver diseases. *Hif1a* can be activated by different mediators in addition to hypoxia, including pro-inflammatory cytokines or oxidative stress, and regulates the activation of the profibrogenic factor TGF- $\beta$ , promoting fibrogenesis. In line with these observations, our results showed that genes related to the regulation of hypoxic response (*Hif1a*), inflammation (*Tnfa*, *Itgax*, *Cd68*), and fibrogenesis (*Col6a1*, *Col6a3*, *Col1a1*) were highly upregulated in the liver of leptin-deficient mice. Furthermore, circulating levels as well as liver expression of TNC were also highly increased in *ob/ob* mice, contributing to inflammation, to the activation of matrix-producing cells, and to matrix deposition and remodeling associated to obesity. According to previous studies from our group, the obese and diabetic phenotype of *ob/ob* mice, as well as the elevated expression of hypoxic, proinflammatory, and profibrotic genes were restored after chronic leptin administration, and may contribute, together with the reduction in lipogenesis and the increase in fatty-acid oxidation, to an improvement of hepatic function. These data support that leptin administration in *ob/ob* mice reverses the conditions of inflammation, fibrogenesis, and extracellular matrix remodeling, normalizing the metabolic status and exerting anti-steatotic effects in the liver. Nonetheless, our data suggest that these phenomena are not exclusively produced by leptin, since similar results were obtained in the pair-fed group, suggesting that other factors might be involved in the beneficial effect observed in the inflammatory and fibrotic response independently of weight

loss [31,47]. In this sense, increased oxidative stress and elevated systemic inflammation constitute a general phenomenon of the obese state, also observed in the context of leptin deficiency [23,48]. The increased levels of pro-inflammatory cytokines observed in *ob/ob* mice may interact with HSCs, inducing collagen gene deposition and hepatic fibrogenesis. Leptin potentiates fibrosis but does not constitute an essential factor for fibrogenesis in the liver.

Excessive fat accumulation in the liver augments ROS formation, inducing the expression of pro-inflammatory genes including TNF- $\alpha$ , IL-6, and cyclooxygenase-2. This, in turn, induces the expression of additional inflammatory mediators that interact with HSCs, increasing the profibrotic response [49]. Although under normal physiological conditions NO is generated constitutively and iNOS expression is absent, different disease conditions, including hepatic fibrosis, induce its expression, mainly in Kupffer cells and HSCs. The excessive NO generation triggers key processes involved in NAFLD progression, including mitochondrial biogenesis and function [50], Kupffer cell polarization [51], and HSC fibrogenesis [52], demonstrating an important role of iNOS in liver inflammation and fibrogenic response [53]. In line with this, *iNOS* deletion significantly reduced the activation of HSCs as confirmed by the reduced gene expression levels of both *Tgfb* and  $\alpha$ -SMA (*Acta2*), suggesting that *iNOS* deficiency could regress the activation of HSC by interfering with the TGF- $\beta$  pathway, protecting from liver fibrosis.

Given that many biological actions of leptin are mediated by NO [15,16,18,20–22], we aimed to evaluate if a functional relationship among them in liver inflammation and fibrosis in the context of obesity. For that purpose, we examined the effects of *iNOS* gene disruption in genetically *ob/ob* mice. We provide evidence, for the first time, that iNOS is involved in liver inflammation and fibrosis linked to leptin deficiency. Several evidences support the improved metabolic profile as well as liver inflammation and fibrosis in the DBKO mice. First of all, a causal relationship between excess fat accumulation, insulin resistance, and progression of hepatic fibrosis is well established [54]. The improved metabolic profile observed in DBKO mice, in line with previous work of our group [22], may constitute an important cornerstone of liver improvement: the decreased accumulation of lipids in hepatocytes together with the increased levels of adiponectin and the reduced liver inflammatory profile in DBKO mice is in accordance with the improved obese and diabetic phenotype of our DBKO model [22].

Moreover, we found that genes involved in inflammation, in the regulation of hypoxic response, and in the excessive collagen deposition are highly enriched in livers of *ob/ob* mice, whereas this upregulation was completely reverted by *iNOS* deletion, similar to previous results described in adipose tissue [22]. Of note, hypoxia induces and regulates iNOS expression, and NO produced by iNOS participates in the stability control of HIF-1 $\alpha$  [55]. In line with these observations, *iNOS* deletion, via decreased transcription and stability of HIF-1 $\alpha$ , might improve liver hypoxia in *ob/ob* mice.

Another important finding of the present study is that the upregulation of osteopontin (*Spp1*) and its receptor *Cd44* observed in *ob/ob* mice was completely prevented by iNOS inhibition. The transmembrane protein CD44 has been recently described as a marker and key player of NASH development [30] and one of the main osteopontin (OPN) receptors [56]. OPN expression is upregulated by proinflammatory cytokines including TNF- $\alpha$  and TGF- $\beta$  and, among other functions, plays a major role in the adipose tissue expansion and in the development of liver stasis [57–59]. It is reported that NO enhances the expression of OPN in the context of hepatic carcinoma associated with high levels of iNOS expression [60]. Our group has previously reported that the absence of OPN reversed HFD-induced fatty liver [57], suggesting that OPN and its corresponding receptor CD44 play a critical role in liver fibrosis, as both are decreased in the absence of the *iNOS* gene. *iNOS* deletion is also related with a profound downregulation of genes encoding collagen, a main structural component of ECM, including *Col61a1*, *Col6a1*, and *Col613*. Besides the regulatory function of NO on *Mmp9* activation [61], the present study demonstrates that *Mmp9* gene expression levels were also significantly reduced in the absence of *iNOS*.

It is necessary to emphasize that *iNOS* ablation significantly reduces circulating levels and liver expression of TNC and its potential role in the stimulation of proinflammatory cytokine expression. Moreover, *iNOS* inhibition also induced a downregulation of basal and leptin-induced *Tnc* transcript levels, suggesting that leptin induces TNC via the activation of the *iNOS* enzyme, with leptin-induced TNC upregulation preventing *iNOS* inhibition.

Collectively, the present study identified a novel relationship for *iNOS* and leptin in mediating liver fibrogenesis. *iNOS* deficiency improves liver inflammation as well as the expression of ECM remodeling-related genes in the context of leptin deficiency, attenuating the development of fibrosis. The weakening of the ECM due to ablation of the *iNOS* gene could be associated with improved insulin sensitivity, reduced inflammation, and metabolic benefits. Moreover, *iNOS* activation induced by leptin is needed and crucial for the synthesis and release of the profibrogenic and proinflammatory TNC, suggesting an important role of this alarmin in the development of hepatic inflammation and fibrosis (Figure 6h). Leptin, together with other important factors involved in increased oxidative stress and elevated systemic inflammation, may contribute to liver steatosis in *ob/ob* mice. Thus, the participation of other factors altered by obesity that impinge on both adipose tissue and liver like fibroblast growth factors (FGFs) should be considered [62]. Further research is needed to discern the specific role of leptin and *iNOS* in liver fibrogenesis.

**Supplementary Materials:** The following are available online at <http://www.mdpi.com/2073-4425/10/3/184/s1>, Figure S1: Gene expression levels of *Cd68* in the liver. Leptin-deficient *ob/ob* mice exhibited a significantly increase in *Cd68* mRNA levels compared to wild type mice, with *iNOS* disruption reducing *Cd68* transcripts levels. Values are mean  $\pm$  SEM (n = 5 per group). The gene expression in WT mice was assumed to be 1. Differences between groups were analyzed by two-way ANOVA. *aP* < 0.05 effect of the absence of the *ob* gene. *bP* < 0.05 effect of the absence of the *iNOS* gene.; Table S1: Sequences of the primers and TaqMan® probes; Table S2: Metabolic characteristics of 12-week-old experimental animals.

**Author Contributions:** S.B., A.R. and G.F. designed the study, collected and analyzed data, wrote the first draft of the manuscript, contributed to discussion, and reviewed the manuscript. J.G.-A., V.C., A.R., B.R. and X.U. collected and analyzed data, contributed to discussion, and reviewed the manuscript. S.B. is guarantor for the contents of the article, had full access to all the data in the study and take responsibility for the integrity of the data and the accuracy of the data analysis.

**Funding:** This work was supported by the Instituto de Salud Carlos III and fondos FEDER (PI16/00221, PI16/01217, PI17/02183 and PI17/02188) and by the Department of Health of Gobierno de Navarra (61/2014). CIBER de Fisiopatología de la Obesidad y Nutrición (CIBEROBN) is an initiative of the Instituto de Salud Carlos III, Spain.

**Conflicts of Interest:** The authors declare that they have no conflict of interest.

## References

- Blond, E.; Disse, E.; Cuerq, C.; Draï, J.; Valette, P.J.; Laville, M.; Thivolet, C.; Simon, C.; Caussy, C. EASL-EASD-EASO clinical practice guidelines for the management of non-alcoholic fatty liver disease in severely obese people: Do they lead to over-referral? *Diabetologia* **2017**, *60*, 1218–1222. [[CrossRef](#)] [[PubMed](#)]
- Chalasanani, N.; Younossi, Z.; Lavine, J.E.; Charlton, M.; Cusi, K.; Rinella, M.; Harrison, S.A.; Brunt, E.M.; Sanyal, A.J. The diagnosis and management of nonalcoholic fatty liver disease: Practice guidance from the American Association for the Study of Liver Diseases. *Hepatology* **2018**, *67*, 328–357. [[CrossRef](#)] [[PubMed](#)]
- Buzzetti, E.; Pinzani, M.; Tsochatzis, E.A. The multiple-hit pathogenesis of non-alcoholic fatty liver disease (NAFLD). *Metabolism* **2016**, *65*, 1038–1048. [[CrossRef](#)] [[PubMed](#)]
- Samuel, V.T.; Liu, Z.X.; Qu, X.; Elder, B.D.; Bilz, S.; Befroy, D.; Romanelli, A.J.; Shulman, G.I. Mechanism of hepatic insulin resistance in non-alcoholic fatty liver disease. *J. Biol. Chem.* **2004**, *279*, 32345–32353. [[CrossRef](#)] [[PubMed](#)]
- Browning, J.D.; Horton, J.D. Molecular mediators of hepatic steatosis and liver injury. *J. Clin. Investig.* **2004**, *114*, 147–152. [[CrossRef](#)] [[PubMed](#)]
- Day, C.P.; James, O.F. Steatohepatitis: A tale of two “hits”? *Gastroenterology* **1998**, *114*, 842–845. [[CrossRef](#)]
- Rolo, A.P.; Teodoro, J.S.; Palmeira, C.M. Role of oxidative stress in the pathogenesis of nonalcoholic steatohepatitis. *Free Radic. Biol. Med.* **2012**, *52*, 59–69. [[CrossRef](#)] [[PubMed](#)]

8. Midwood, K.S.; Hussenet, T.; Langlois, B.; Orend, G. Advances in tenascin-C biology. *Cell Mol. Life Sci.* **2011**, *68*, 3175–3199. [[CrossRef](#)] [[PubMed](#)]
9. El-Karef, A.; Yoshida, T.; Gabazza, E.C.; Nishioka, T.; Inada, H.; Sakakura, T.; Imanaka-Yoshida, K. Deficiency of tenascin-C attenuates liver fibrosis in immune-mediated chronic hepatitis in mice. *J. Pathol.* **2007**, *211*, 86–94. [[CrossRef](#)] [[PubMed](#)]
10. Van Eyken, P.; Sciot, R.; Desmet, V.J. Expression of the novel extracellular matrix component tenascin in normal and diseased human liver. An immunohistochemical study. *J. Hepatol.* **1990**, *11*, 43–52. [[CrossRef](#)]
11. Marra, F. Leptin and liver fibrosis: A matter of fat. *Gastroenterology* **2002**, *122*, 1529–1532. [[CrossRef](#)] [[PubMed](#)]
12. Bertolani, C.; Marra, F. Role of adipocytokines in hepatic fibrosis. *Curr. Pharm. Des.* **2010**, *16*, 1929–1940. [[CrossRef](#)] [[PubMed](#)]
13. Rodríguez, A.; Ezquerro, S.; Méndez-Gimenez, L.; Becerril, S.; Frühbeck, G. Revisiting the adipocyte: A model for integration of cytokine signaling in the regulation of energy metabolism. *Am. J. Physiol. Endocrinol. Metab.* **2015**, *309*, E691–E714. [[CrossRef](#)] [[PubMed](#)]
14. Gómez-Ambrosi, J.; Salvador, J.; Paramo, J.A.; Orbe, J.; de Irala, J.; Díez-Caballero, A.; Gil, M.J.; Cienfuegos, J.A.; Frühbeck, G. Involvement of leptin in the association between percentage of body fat and cardiovascular risk factors. *Clin. Biochem.* **2002**, *35*, 315–320. [[CrossRef](#)]
15. Frühbeck, G. Pivotal role of nitric oxide in the control of blood pressure after leptin administration. *Diabetes* **1999**, *48*, 903–908. [[CrossRef](#)] [[PubMed](#)]
16. Frühbeck, G.; Gómez-Ambrosi, J. Modulation of the leptin-induced white adipose tissue lipolysis by nitric oxide. *Cell Signal.* **2001**, *13*, 827–833. [[CrossRef](#)]
17. Rodríguez, A.; Fortuño, A.; Gómez-Ambrosi, J.; Zalba, G.; Díez, J.; Frühbeck, G. The inhibitory effect of leptin on angiotensin II-induced vasoconstriction in vascular smooth muscle cells is mediated via a nitric oxide-dependent mechanism. *Endocrinology* **2007**, *148*, 324–331.
18. Becerril, S.; Rodríguez, A.; Catalán, V.; Sáinz, N.; Ramírez, B.; Collantes, M.; Peñuelas, I.; Gómez-Ambrosi, J.; Frühbeck, G. Deletion of inducible nitric-oxide synthase in leptin-deficient mice improves brown adipose tissue function. *PLoS ONE* **2010**, *5*, e10962. [[CrossRef](#)] [[PubMed](#)]
19. Frühbeck, G.; Gómez-Ambrosi, J.; Salvador, J. Leptin-induced lipolysis opposes the tonic inhibition of endogenous adenosine in white adipocytes. *FASEB J.* **2001**, *15*, 333–340. [[CrossRef](#)] [[PubMed](#)]
20. Shiuchi, T.; Nakagami, H.; Iwai, M.; Takeda, Y.; Cui, T.; Chen, R.; Minokoshi, Y.; Horiuchi, M. Involvement of bradykinin and nitric oxide in leptin-mediated glucose uptake in skeletal muscle. *Endocrinology* **2001**, *142*, 608–612. [[CrossRef](#)] [[PubMed](#)]
21. Dixit, V.D.; Mielenz, M.; Taub, D.D.; Parvizi, N. Leptin induces growth hormone secretion from peripheral blood mononuclear cells via a protein kinase C- and nitric oxide-dependent mechanism. *Endocrinology* **2003**, *144*, 5595–5603. [[CrossRef](#)] [[PubMed](#)]
22. Becerril, S.; Rodríguez, A.; Catalán, V.; Méndez-Gimenez, L.; Ramírez, B.; Sainz, N.; Llorente, M.; Unamuno, X.; Gómez-Ambrosi, J.; Frühbeck, G. Targeted disruption of the *iNOS* gene improves adipose tissue inflammation and fibrosis in leptin-deficient *ob/ob* mice: Role of tenascin C. *Int. J. Obes. (Lond.)* **2018**, *42*, 1458–1470. [[CrossRef](#)] [[PubMed](#)]
23. Sainz, N.; Rodríguez, A.; Catalán, V.; Becerril, S.; Ramírez, B.; Gómez-Ambrosi, J.; Frühbeck, G. Leptin administration downregulates the increased expression levels of genes related to oxidative stress and inflammation in the skeletal muscle of *ob/ob* mice. *Mediat. Inflamm.* **2010**, *2010*, 784343. [[CrossRef](#)] [[PubMed](#)]
24. Frühbeck, G.; Alonso, R.; Marzo, F.; Santidrián, S. A modified method for the indirect quantitative analysis of phytate in foodstuffs. *Anal. Biochem.* **1995**, *225*, 206–212.
25. Rodríguez, A.; Catalán, V.; Gómez-Ambrosi, J.; García-Navarro, S.; Rotellar, F.; Valentí, V.; Silva, C.; Gil, M.J.; Salvador, J.; Burrell, M.A.; et al. Insulin- and leptin-mediated control of aquaglyceroporins in human adipocytes and hepatocytes is mediated via the PI3K/Akt/mTOR signaling cascade. *J. Clin. Endocrinol. Metab.* **2011**, *96*, E586–E597. [[CrossRef](#)] [[PubMed](#)]
26. Catalán, V.; Gómez-Ambrosi, J.; Rodríguez, A.; Silva, C.; Rotellar, F.; Gil, M.J.; Cienfuegos, J.A.; Salvador, J.; Frühbeck, G. Expression of caveolin-1 in human adipose tissue is upregulated in obesity and obesity-associated type 2 diabetes mellitus and related to inflammation. *Clin. Endocrinol. (Oxf.)* **2008**, *68*, 213–219. [[CrossRef](#)] [[PubMed](#)]

27. Catalán, V.; Gómez-Ambrosi, J.; Rotellar, F.; Silva, C.; Rodríguez, A.; Salvador, J.; Gil, M.J.; Cienfuegos, J.A.; Frühbeck, G. Validation of endogenous control genes in human adipose tissue: Relevance to obesity and obesity-associated type 2 diabetes mellitus. *Horm. Metab. Res.* **2007**, *39*, 495–500. [[CrossRef](#)] [[PubMed](#)]
28. Halberg, N.; Khan, T.; Trujillo, M.E.; Wernstedt-Asterholm, I.; Attie, A.D.; Sherwani, S.; Wang, Z.V.; Landskroner-Eiger, S.; Dineen, S.; Magalang, U.J.; et al. Hypoxia-inducible factor 1a induces fibrosis and insulin resistance in white adipose tissue. *Mol. Cell Biol.* **2009**, *29*, 4467–4483. [[CrossRef](#)] [[PubMed](#)]
29. Koyama, Y.; Brenner, D.A. Liver inflammation and fibrosis. *J. Clin. Investig.* **2017**, *127*, 55–64. [[CrossRef](#)] [[PubMed](#)]
30. Patouraux, S.; Rousseau, D.; Bonnafous, S.; Lebeaupin, C.; Luci, C.; Canivet, C.M.; Schenck, A.S.; Bertola, A.; Saint-Paul, M.C.; Iannelli, A.; Gugenheim, J.; et al. CD44 is a key player in non-alcoholic steatohepatitis. *J. Hepatol.* **2017**, *67*, 328–338. [[CrossRef](#)] [[PubMed](#)]
31. Sáinz, N.; Rodríguez, A.; Catalán, V.; Becerril, S.; Ramírez, B.; Gómez-Ambrosi, J.; Frühbeck, G. Leptin administration favors muscle mass accretion by decreasing FoxO3a and increasing PGC-1a in *ob/ob* mice. *PLoS ONE* **2009**, *4*, e6808. [[CrossRef](#)] [[PubMed](#)]
32. Halaas, J.L.; Gajiwala, K.S.; Maffei, M.; Cohen, S.L.; Chait, B.T.; Rabinowitz, D.; Lallone, R.L.; Burley, S.K.; Friedman, J.M. Weight-reducing effects of the plasma protein encoded by the obese gene. *Science* **1995**, *269*, 543–546. [[CrossRef](#)] [[PubMed](#)]
33. Pellemounter, M.A.; Cullen, M.J.; Baker, M.B.; Hecht, R.; Winters, D.; Boone, T.; Collins, F. Effects of the obese gene product on body weight regulation in *ob/ob* mice. *Science* **1995**, *269*, 540–543. [[CrossRef](#)] [[PubMed](#)]
34. Frühbeck, G.; Gómez-Ambrosi, J. Control of body weight: A physiologic and transgenic perspective. *Diabetologia* **2003**, *46*, 143–172. [[CrossRef](#)] [[PubMed](#)]
35. Petersen, K.F.; Oral, E.A.; Dufour, S.; Befroy, D.; Ariyan, C.; Yu, C.; Cline, G.W.; DePaoli, A.M.; Taylor, S.I.; Gorden, P.; et al. Leptin reverses insulin resistance and hepatic steatosis in patients with severe lipodystrophy. *J. Clin. Investig.* **2002**, *109*, 1345–1350. [[CrossRef](#)] [[PubMed](#)]
36. Polyzos, S.A.; Aronis, K.N.; Kountouras, J.; Raptis, D.D.; Vasiloglou, M.F.; Mantzoros, C.S. Circulating leptin in non-alcoholic fatty liver disease: A systematic review and meta-analysis. *Diabetologia* **2016**, *59*, 30–43. [[CrossRef](#)] [[PubMed](#)]
37. Muruzábal, F.J.; Frühbeck, G.; Gómez-Ambrosi, J.; Archanco, M.; Burrell, M.A. Immunocytochemical detection of leptin in non-mammalian vertebrate stomach. *Gen. Comp. Endocrinol.* **2002**, *128*, 149–152. [[CrossRef](#)]
38. Polyzos, S.A.; Kountouras, J.; Zavos, C.; Deretzi, G. The potential adverse role of leptin resistance in nonalcoholic fatty liver disease: A hypothesis based on critical review of the literature. *J. Clin. Gastroenterol.* **2011**, *45*, 50–54. [[CrossRef](#)] [[PubMed](#)]
39. Perugorria, M.J.; Wilson, C.L.; Zeybel, M.; Walsh, M.; Amin, S.; Robinson, S.; White, S.A.; Burt, A.D.; Oakley, F.; Tsukamoto, H.; et al. Histone methyltransferase ASH1 orchestrates fibrogenic gene transcription during myofibroblast transdifferentiation. *Hepatology* **2012**, *56*, 1129–1139. [[CrossRef](#)] [[PubMed](#)]
40. Tang, L.Y.; Heller, M.; Meng, Z.; Yu, L.R.; Tang, Y.; Zhou, M.; Zhang, Y.E. Transforming Growth Factor- $\beta$  (TGF- $\beta$ ) Directly Activates the JAK1-STAT3 Axis to Induce Hepatic Fibrosis in Coordination with the SMAD Pathway. *J. Biol. Chem.* **2017**, *292*, 4302–4312. [[CrossRef](#)] [[PubMed](#)]
41. Shen, J.; Sakaida, I.; Uchida, K.; Terai, S.; Okita, K. Leptin enhances TNF- $\alpha$  production via p38 and JNK MAPK in LPS-stimulated Kupffer cells. *Life Sci.* **2005**, *77*, 1502–1515. [[CrossRef](#)] [[PubMed](#)]
42. Faggioni, R.; Jones-Carson, J.; Reed, D.A.; Dinarello, C.A.; Feingold, K.R.; Grunfeld, C.; Fantuzzi, G. Leptin-deficient (*ob/ob*) mice are protected from T cell-mediated hepatotoxicity: Role of tumor necrosis factor  $\alpha$  and IL-18. *Proc. Natl. Acad. Sci. USA* **2000**, *97*, 2367–2372. [[CrossRef](#)] [[PubMed](#)]
43. Schwabe, R.F.; Seki, E.; Brenner, D.A. Toll-like receptor signaling in the liver. *Gastroenterology* **2006**, *130*, 1886–1900. [[CrossRef](#)] [[PubMed](#)]
44. Midwood, K.; Sacre, S.; Piccinini, A.M.; Inglis, J.; Trebaul, A.; Chan, E.; Sofat, N.; Kashiwagi, M.; Orend, G. Tenascin-C is an endogenous activator of Toll-like receptor 4 that is essential for maintaining inflammation in arthritic joint disease. *Nat. Med.* **2009**, *15*, 774–780. [[CrossRef](#)] [[PubMed](#)]
45. Bhattacharyya, S.; Wang, W.; Morales-Nebreda, L.; Feng, G.; Wu, M.; Zhou, X.; Lafyatis, R.; Lee, J.; Hinchcliff, M.; Feghali-Bostwick, C.; et al. Tenascin-C drives persistence of organ fibrosis. *Nat. Commun.* **2016**, *7*, 11703. [[CrossRef](#)] [[PubMed](#)]



46. Pérez-Pérez, A.; Vilarino-García, T.; Fernández-Riejos, P.; Martín-González, J.; Segura-Egea, J.J.; Sánchez-Margalet, V. Role of leptin as a link between metabolism and the immune system. *Cytokine Growth Factor Rev.* **2017**, *35*, 71–84. [[CrossRef](#)] [[PubMed](#)]
47. Cousin, B.; Bascands-Viguerie, N.; Kassis, N.; Nibbelink, M.; Ambid, L.; Casteilla, L.; Pénicaud, L. Cellular changes during cold acclimation in adipose tissues. *J. Cell Physiol.* **1996**, *167*, 285–289. [[CrossRef](#)]
48. Bankoglu, E.E.; Seyfried, F.; Rotzinger, L.; Nordbeck, A.; Corteville, C.; Jurowich, C.; Germer, C.T.; Otto, C.; Stopper, H.; et al. Impact of weight loss induced by gastric bypass or caloric restriction on oxidative stress and genomic damage in obese Zucker rats. *Free Radic. Biol. Med.* **2016**, *94*, 208–217. [[CrossRef](#)] [[PubMed](#)]
49. Saxena, N.K.; Anania, F.A. Adipocytokines and hepatic fibrosis. *Trends Endocrinol. Metab.* **2015**, *26*, 153–161. [[CrossRef](#)] [[PubMed](#)]
50. Nisoli, E.; Clementi, E.; Paolucci, C.; Cozzi, V.; Tonello, C.; Sciorati, C.; Bracale, R.; Valerio, A.; Francolini, M.; Moncada, S.; et al. Mitochondrial biogenesis in mammals: The role of endogenous nitric oxide. *Science* **2003**, *299*, 896–899. [[CrossRef](#)] [[PubMed](#)]
51. Tateya, S.; Rizzo, N.O.; Handa, P.; Cheng, A.M.; Morgan-Stevenson, V.; Daum, G.; Clowes, A.W.; Morton, G.J.; Schwartz, M.W.; Kim, F. Endothelial NO/cGMP/VASP signaling attenuates Kupffer cell activation and hepatic insulin resistance induced by high-fat feeding. *Diabetes* **2011**, *60*, 2792–2801. [[CrossRef](#)] [[PubMed](#)]
52. Xie, G.; Wang, X.; Wang, L.; Atkinson, R.D.; Kanel, G.C.; Gaarde, W.A.; Deleve, L.D. Role of differentiation of liver sinusoidal endothelial cells in progression and regression of hepatic fibrosis in rats. *Gastroenterology* **2012**, *142*, 918.e6–927.e6. [[CrossRef](#)] [[PubMed](#)]
53. Anavi, S.; Eisenberg-Bord, M.; Hahn-Obercyger, M.; Genin, O.; Pines, M.; Tirosch, O. The role of iNOS in cholesterol-induced liver fibrosis. *Lab. Investig.* **2015**, *95*, 914–924. [[CrossRef](#)] [[PubMed](#)]
54. Hui, J.M.; Hodge, A.; Farrell, G.C.; Kench, J.G.; Kriketos, A.; George, J. Beyond insulin resistance in NASH: TNF-alpha or adiponectin? *Hepatology* **2004**, *40*, 46–54. [[CrossRef](#)] [[PubMed](#)]
55. Brune, B.; Zhou, J. Hypoxia-inducible factor-1a under the control of nitric oxide. *Methods Enzymol.* **2007**, *435*, 463–478. [[PubMed](#)]
56. Scatena, M.; Liaw, L.; Giachelli, C.M. Osteopontin: A multifunctional molecule regulating chronic inflammation and vascular disease. *Arterioscler. Thromb. Vasc. Biol.* **2007**, *27*, 2302–2309. [[CrossRef](#)] [[PubMed](#)]
57. Lancha, A.; Rodríguez, A.; Catalán, V.; Becerril, S.; Sainz, N.; Ramírez, B.; Burrell, M.A.; Salvador, J.; Frühbeck, G.; Gómez-Ambrosi, J. Osteopontin deletion prevents the development of obesity and hepatic steatosis via impaired adipose tissue matrix remodeling and reduced inflammation and fibrosis in adipose tissue and liver in mice. *PLoS ONE* **2014**, *9*, e98398. [[CrossRef](#)] [[PubMed](#)]
58. Wen, Y.; Jeong, S.; Xia, Q.; Kong, X. Role of Osteopontin in Liver Diseases. *Int. J. Biol. Sci.* **2016**, *12*, 1121–1128. [[CrossRef](#)] [[PubMed](#)]
59. Nagoshi, S. Osteopontin: Versatile modulator of liver diseases. *Hepatol. Res. Off. J. Jpn. Soc. Hepatol.* **2014**, *44*, 22–30. [[CrossRef](#)] [[PubMed](#)]
60. Guo, H.; Marroquin, C.E.; Wai, P.Y.; Kuo, P.C. Nitric oxide-dependent osteopontin expression induces metastatic behavior in HepG2 cells. *Dig. Dis. Sci.* **2005**, *50*, 1288–1298. [[CrossRef](#)] [[PubMed](#)]
61. Hamada, T.; Duarte, S.; Tsuchihashi, S.; Busuttil, R.W.; Coito, A.J. Inducible nitric oxide synthase deficiency impairs matrix metalloproteinase-9 activity and disrupts leukocyte migration in hepatic ischemia/reperfusion injury. *Am. J. Pathol.* **2009**, *174*, 2265–2277. [[CrossRef](#)] [[PubMed](#)]
62. Gallego-Escuredo, J.M.; Gómez-Ambrosi, J.; Catalán, V.; Domingo, P.; Giral, M.; Frühbeck, G.; Villarroja, F. Opposite alterations in FGF21 and FGF19 levels and disturbed expression of the receptor machinery for endocrine FGFs in obese patients. *Int. J. Obes. (Lond.)* **2015**, *39*, 121–129. [[CrossRef](#)] [[PubMed](#)]

